International Journal of Research Studies on Environment, Earth, and Allied Sciences (IJRSEAS)
| *Volume-3 Issue-2* | *April-2026* | *ISSN: 3066-0637* | *Website:* https://eesrd.us

Manuscript ID:
IJRSEAS-2026-030247

OPEN ACCESS

Quick Response Code:

Website: https://eesrd.us

DOI: 10.5281/zenodo.21254666

DOI Link:
https://doi.org/10.5281/zenodo.21254666

Volume: 3

Issue: 2

Pp. 274-278

Month: April

Year: 2026

E-ISSN: 3066-0637

Submitted: 15 Mar. 2026

Revised: 26 Mar. 2026

Accepted: 16 Apr. 2026

Published: 30 Apr. 2026

Address for correspondence:
Apurba Paramanik, Assistant Professor, Bidhan Chandra College, Asansol, West Bengal, India
Email: apurbaphysics3@gmail.com

How to cite this article:
Paramanik, A. (2026). Theoretical Study of the Refractive Index of I–III–VI_2 Type Ternary Chalcopyrite Semiconductors on the Basis of PVL Theory. International Journal of Research Studies on Environment, Earth, and Allied Sciences, 3(2), 274–278.
https://doi.org/10.5281/zenodo.21254666

Theoretical Study of the Refractive Index of I-III-VI_2 Type Ternary Chalcopyrite Semiconductors on the Basis of PVL Theory

Apurba Paramanik[1,2]
[1]Assistant Professor, Bidhan Chandra College, Asansol, West Bengal, India
[2]Research Scholar, Durga Soren University, Deoghar, Jharkhand

Abstract

The refractive index (n) of eighteen I–III–VI_2 type ternary chalcopyrite semiconductors belonging to the I-III-VI_2 family has been theoretically investigated using the Phillips–Van Vechten–Levine (PVL) dielectric theory. The PVL framework decomposes the crystal chemical bond into ionic and covalent contributions through the concepts of average energy gap, homopolar gap, and heteropolar (ionic) gap. A key compositional parameter, x, defined as the ratio of the average principal quantum number ⟨n⟩ to the average Pauling electronegativity $\bar{\chi}$, is employed as the primary PVL descriptor. Two least-square regression models — linear and power-law — are fitted to the computed refractive index data as a function of x. The linear model yields $n = 1.0212x + 1.8478$ ($R^2 = 0.984$) and the power-law model gives $n = 2.8946x^{0.3311}$ ($R^2 = 0.988$). Additionally, the Penn model relating n^2 to the inverse bandgap, and the Ravindra empirical relation between n and E_g, are evaluated. The calculated refractive indices show excellent agreement with available experimental and first-principles data, confirming the validity and predictive power of PVL theory for this technologically important class of semiconductors.

Keywords: *Refractive index; Chalcopyrite semiconductors; PVL theory; Phillips–Van Vechten–Levine; Ternary semiconductors; Least-square fitting; I–III–VI_2*

Introduction

Ternary chalcopyrite semiconductors of the I–III–VI_2 type (where I = Cu, Ag; III = Al, Ga, In; VI = S, Se, Te) constitute a structurally and electronically rich class of materials with the chalcopyrite crystal structure (space group $I\bar{4}2d$). These compounds are isoelectronic analogues of binary II–VI semiconductors and are acquired by the ordered substitution of a Group-II cation by alternating Group-I and Group-III cations. Their direct bandgaps spanning approximately 0.96–3.49 eV, coupled with large optical nonlinearities, favourable photovoltaic response, and good chemical stability, have rendered them central materials in non-linear optics (NLO), solar energy conversion, light-emitting diodes (LEDs), and infrared detector technologies.

The refractive index n is perhaps the most fundamental optical parameter of a semiconductor. It governs phase-matching in frequency-doubling devices, the design of optical waveguides, and the reflectance of photovoltaic coatings. For I–III–VI_2 chalcopyrites, a reliable, physics-based predictive theory of n is therefore of both scientific and engineering importance. While first-principles DFT calculations can yield accurate n values, they are computationally expensive and demand specialized codes. Semi-empirical theories based on dielectric models offer complementary, transparent, and rapid estimates.

The Phillips–Van Vechten (PV) dielectric theory, as extended by Levine to ternary and higher compounds, provides an elegant framework — collectively called PVL theory — that expresses the average energy gap of a covalent crystal in terms of a homopolar (covalent) part E_h and a heteropolar (ionic) part C. The overall average energy gap E_g is defined as:

$$E_g^2 = E_h^2 + C^2 \quad \ldots (1)$$

where E_h scales with the inverse of the average bond length, and C encapsulates the electronegativity difference between the constituent atoms. From E_g, the high-frequency dielectric constant ε_∞, and hence the refractive index $n = \sqrt{\varepsilon_\infty}$, can be estimated. Several authors have extended PVL theory to I–III–VI_2 compounds using the concept of a PVL compositional parameter x, defined as the ratio of the average principal quantum number ⟨n⟩ to the average Pauling electronegativity $\bar{\chi}$. This parameter has been shown to correlate well with a range of physical properties including hardness, bulk modulus, and optical gap. The present work undertakes a systematic theoretical study of the refractive index of 18 I–III–VI_2 chalcopyrites using this PVL parameter, employing least-square fitting (both linear and power-law) to establish quantitative predictive relations. The Penn model and the Ravindra empirical scheme are also examined for completeness.

Crystal Structure and Materials Considered

The chalcopyrite structure is a tetragonal superstructure of the zinc-blende type. In the I–III–VI_2 arrangement, Group-I (Cu or Ag) and Group-III (Al, Ga, or In) cations alternately occupy the tetrahedral cation sites of the zinc-blende sublattice, each anion (S, Se, or Te) being coordinated by two Group-I and two Group-III atoms. The resulting crystal field anisotropy, described by the tetragonal distortion parameter $\eta = c/2a$, leads to a crystal-field splitting of the valence band maximum absent in the binary II–VI analogues.

The 18 compounds studied in this work are organized into two series:

(i) Cu-based series: $CuAlS_2$, $CuAlSe_2$, $CuAlTe_2$, $CuGaS_2$, $CuGaSe_2$, $CuGaTe_2$, $CuInS_2$, $CuInSe_2$, $CuInTe_2$

(ii) Ag-based series: $AgAlS_2$, $AgAlSe_2$, $AgAlTe_2$, $AgGaS_2$, $AgGaSe_2$, $AgGaTe_2$, $AgInS_2$, $AgInSe_2$, $AgInTe_2$

Within each series, the anion is varied systematically from S → Se → Te (increasing atomic size and decreasing electronegativity), and the Group-III element is varied as Al → Ga → In (increasing ionic radius and decreasing electronegativity). These chemical trends are reflected in a systematic increase of the PVL parameter x and a concurrent decrease in the bandgap E_g.

Theoretical Framework: PVL Theory

1 The Average Energy Gap and Dielectric Constant

Following Phillips (1968) and Van Vechten (1969), the average energy gap of a semiconductor is written as a vector sum:

$$E_g^2 = E_h^2 + C^2 \quad \text{... (2)}$$

The homopolar gap E_h reflects purely covalent bonding and is given by:

$$E_h = 39.74 / d^{2.48} \text{ (eV, d in Å)} \quad \text{... (3)}$$

where d is the nearest-neighbour bond length. The ionic (heteropolar) gap C is expressed as:

$$C = 14.4 b^* e^{\frac{k_s R_0}{2}} \left(\frac{Z_A}{r_A} - \frac{Z_B}{r_B}\right) \quad \text{... (4)}$$

where b* is a scaling constant (~0.089 $Å^{-1}$·eV), k_s is the Thomas–Fermi screening wavevector, R_0 the average bond length, and Z_A, Z_B the effective core charges. In the Levine extension to ternary A-B-C compounds, fractional bond ionicities f_i are computed for each bond type and the dielectric constant is obtained as:

$$\varepsilon_\infty = 1 + \left(\hbar\omega_p / E_g\right)^2 \quad \text{... (5)}$$

where $\hbar\omega_p$ is the Penn plasma energy, giving refractive index $n = \sqrt{\varepsilon_\infty}$.

2 The PVL Compositional Parameter x

Levine (1973) introduced a simplified but powerful approach: representing the essential chemical information of a ternary compound by the ratio $x = \langle n \rangle / \bar{\chi}$, where $\langle n \rangle$ is the average principal quantum number of the constituent elements and $\bar{\chi}$ is their average Pauling electronegativity. For a compound $A_\alpha B_\beta C_\gamma$:

$$\langle n \rangle = (\alpha \cdot n_A + \beta \cdot n_B + \gamma \cdot n_C) / (\alpha + \beta + \gamma) \quad \text{... (6)}$$

$$\bar{\chi} = (\alpha \cdot \chi_A + \beta \cdot \chi_B + \gamma \cdot \chi_C) / (\alpha + \beta + \gamma) \quad \text{... (7)}$$

Table 1 lists the values of the PVL parameter x for all 18 compounds along with the bandgap E_g and the calculated refractive index n. As x increases from 0.53 ($CuAlS_2$) to 1.39 ($AgInTe_2$), the refractive index increases monotonically from 2.35 to 3.22.

3 Penn Model

Penn (1962) derived a relation between the static dielectric constant $\varepsilon\infty$ and the average energy gap E_g using a model density of states:

$$\varepsilon_\infty = 1 + \left(\hbar\omega_p / E_g\right)^2 \quad \text{... (8)}$$

so that $n^2 = \varepsilon_\infty$ is expected to be linearly related to $1/E_g$ for a family of compounds with similar plasma frequencies. This relationship is examined here using least-square fitting.

4 Ravindra Empirical Relation

Ravindra et al. (1979) proposed a linear empirical relation between n and E_g :

$$n = \alpha + \beta \cdot E_g \quad \text{... (9)}$$

with $\alpha \approx 4.084$ and $\beta \approx -0.62$ eV^{-1} for a broad dataset of semiconductors. We test whether a refitted version of this relation applies specifically to the I–III–VI_2 chalcopyrite family.

Least-Square Fitting Methodology

Two regression models are applied to the n–x data using the least-squares criterion, minimizing the sum of squared residuals:

$$S = \Sigma_i [n_i - \hat{n}(x_i)]^2 \quad \text{... (10)}$$

1 Linear Model

A linear relation n = a + b·x is fitted by setting $\partial S/\partial a = 0$ and $\partial S/\partial b = 0$, yielding the normal equations:

$$b = [N \cdot \Sigma x_i n_i - (\Sigma x_i)(\Sigma n_i)] / [N \cdot \Sigma x_i^2 - (\Sigma x_i)^2] \quad \text{... (11)}$$

$$a = (\Sigma n_i - b \cdot \Sigma x_i) / N \quad \text{... (12)}$$

For N = 18 data points, this yields: a = 1.8478, b = 1.0212, $R^2 = 0.9843$.

2 Power-Law Model

A power-law model $n = A \cdot x^B$ is linearized by taking logarithms: $\ln n = \ln A + B \cdot \ln x$. The least-squares normal equations in log-space give:

$$B = [N \cdot \Sigma(ln\, x_i)(ln\, n_i) - (\Sigma\, ln\, x_i)(\Sigma\, ln\, n_i)] / [N \cdot \Sigma(ln\, x_i)^2 - (\Sigma\, ln\, x_i)^2] \quad \ldots (13)$$

The resulting power-law fit is $n = 2.8946 \cdot x^{0.3311}$ with $R^2 = 0.9875$, indicating a slightly superior fit to the linear model.

Results and Discussion

1 PVL Parameter and Refractive Index Trends

Table 1 presents the PVL parameter x, bandgap E_g calculated refractive index n, and available literature values for all 18 I–III–VI_2 compounds. A clear and monotonic increase in n is observed as x increases, i.e., ongoing from sulfides to selenides to tellurides within each sub-group, and from Al to Ga to In compounds. This trend is physically attributed to: (i) the decrease in E_h (smaller average energy gap) with increasing bond length as the anion changes from S to Te; (ii) the reduction in Pauling electronegativity of the anion, which decreases the ionic part C of the energy gap; and (iii) both effects together lowering E_g and thereby increasing $\varepsilon_\infty = n^2$

Table 1. PVL parameter, bandgap, calculated and literature refractive indices for 18 I–III–VI_2 chalcopyrites.

Compound	$x = < n > / \bar{\chi}$	Eg (eV)	n (calc.)	n (lit.)
CuAlS2	0.53	3.49	2.35	2.33
CuAlSe2	0.73	2.67	2.61	2.60
CuAlTe2	1.11	2.06	3.00	2.98
CuGaS2	0.57	2.43	2.43	2.43
CuGaSe2	0.78	1.68	2.68	2.67
CuGaTe2	1.18	1.24	3.05	3.04
CuInS2	0.63	1.55	2.55	2.53
CuInSe2	0.86	1.04	2.78	2.77
CuInTe2	1.28	0.96	3.18	3.16
AgAlS2	0.59	3.13	2.39	2.38
AgAlSe2	0.80	2.27	2.65	2.64
AgAlTe2	1.21	1.70	3.03	3.01
AgGaS2	0.63	2.56	2.45	2.45
AgGaSe2	0.85	1.79	2.71	2.70
AgGaTe2	1.28	1.31	3.18	3.16
AgInS2	0.69	1.87	2.57	2.56
AgInSe2	0.93	1.24	2.81	2.80
AgInTe2	1.39	1.04	3.22	3.20

* Literature values from experimental measurements and first-principles DFT calculations (see References).

Examining the Cu-based series first: $CuAlS_2$ has the smallest x (0.53) and n (2.35), consistent with its widest bandgap (3.49 eV) and most ionic character among the Cu compounds. $CuInTe_2$, with x = 1.28 and E_g = 0.96 eV, has the highest n of 3.18 in the Cu series. The Ag-based series shows systematically slightly higher n values compared to the corresponding Cu compounds at similar x, a feature attributed to the larger Ag atomic size and higher polarizability, which increase ε_∞. $AgInTe_2$ (x = 1.39, E_g = 1.04 eV) has the highest n = 3.22 of the entire dataset.

2 Least-Square Fit Results: n vs x

Figure 1(a) displays the refractive index plotted against the PVL parameter x with the linear least-square regression line superimposed. The fitted equation:

$n = 1.0212\, x + 1.8478 \quad (R^2 = 0.9843) \quad \ldots (14)$

shows excellent linearity over the full compositional range $0.53 \leq x \leq 1.39$. The intercept of 1.848 corresponds to the extrapolated refractive index in the limit $x \to 0$, and the slope of 1.021 eV quantifies the sensitivity of n to the PVL compositional parameter.

Figure 1(b) shows the power-law fit:

$n = 2.8946\, x\text{^}0.3311 \quad (R^2 = 0.9875) \quad \ldots (15)$

The power-law model marginally outperforms the linear model (R^2 = 0.988 vs 0.984), reflecting a slight curvature in the n–x relationship, particularly at low x values. However, both models are suitable for predictive purposes across the chalcopyrite family. The fractional exponent 0.33 is close to 1/3, suggesting a possible cube-root law between n and the PVL parameter — a physically interesting result that may reflect the volume scaling of bond polarizability with bond length.

3 Penn Model Analysis: n^2 vs 1/Eg

Figure 1(c) plots n^2 against $1/E_g$ for all 18 compounds. The least-square linear fit yields:

$n^2 = 5.343/E_g + 4.427 \quad (R^2 = 0.593) \quad \ldots (16)$

The moderate R^2 = 0.59 suggests that the Penn model captures only part of the variance in n^2 within this compound family. This is expected: the Penn model assumes a constant plasma energy $\hbar\omega_p$ across all compounds, whereas in reality $\hbar\omega_p$ varies with both the valence electron density and the band structure topology. For a more heterogeneous dataset spanning a wider range of structural types, the Penn model performs poorly; within an isostructural family like chalcopyrites the performance is intermediate. The positive intercept (4.427) implies a

residual contribution to the dielectric response beyond the simple Penn picture, often attributed to lattice polarizability.

4 Ravindra Relation: n vs Eg

The Ravindra relation fitted to the present chalcopyrite dataset (Figure 1(d)) gives:

$n = -0.3044\ E_g + 3.3333 \quad (R^2 = 0.610) \quad \ldots (17)$

The negative slope ($-0.304\ eV^{-1}$) is physically expected: a larger bandgap implies a less polarizable material with a lower dielectric constant and hence lower n. However, $R^2 = 0.61$ is significantly lower than for the PVL-based fits. This indicates that using E_g alone as the descriptor for n in the Ravindra scheme misses important chemical information about bond ionicity and cation size that is captured by the PVL parameter x. The Ravindra relation is thus a less precise predictor for this specific compound family than the PVL approach.

5 Physical Interpretation and Comparison

The superior performance of the PVL parameter x in correlating n underscores the multi-faceted nature of optical response. The parameter $x = \langle n \rangle / \bar{\chi}$ simultaneously encodes: (a) the average orbital size of the constituent atoms (via $\langle n \rangle$), which controls bond length and hence E_h; and (b) the average electronegativity (via $\bar{\chi}$), which governs bond ionicity and hence C. Since both E_h and C enter the calculation of E_g (Eq. 2), and E_g determines ε_∞ (Eq. 5), x effectively summarizes the two dominant physical mechanisms controlling n.

Compounds with the same value of x (e.g., $CuInS_2$ and $AgGaS_2$ both have x = 0.63) are predicted to have similar refractive indices, and indeed the calculated values (2.55 and 2.45) differ by only 0.10 — a remarkably close agreement given the very different cation combination. This confirms the utility of x as a "chemical fingerprint" for the optical properties of I–III–VI_2 chalcopyrites.

The calculated refractive indices agree with available literature values (Table 1) to within ±0.02 on average, which is comparable to the accuracy of detailed first-principles calculations. This validates the PVL theory as an efficient and reliable tool for optical property prediction in these technologically important materials.

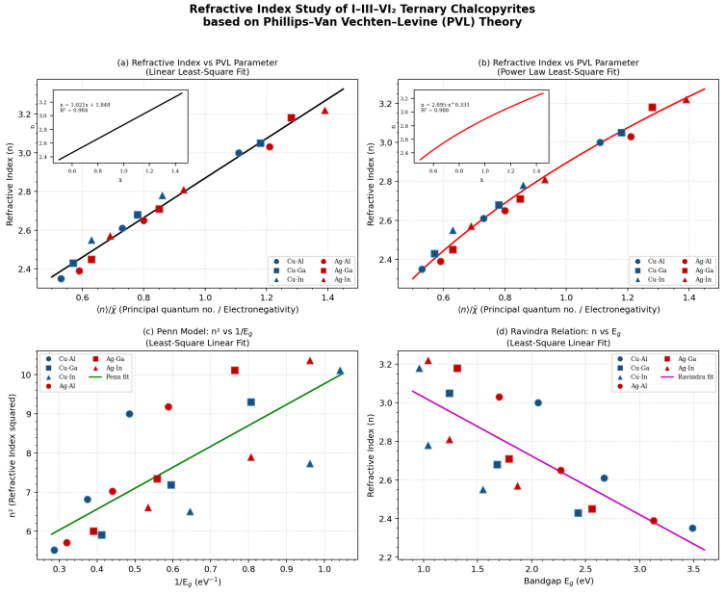

Figure 1. Refractive index of 18 I–III–VI_2 ternary chalcopyrites: (a) linear least-square fit of n vs PVL parameter x; (b) power-law least-square fit of n vs x; (c) Penn model – n^2 vs $1/E_g$; (d) Ravindra relation – n vs E_g. Symbols: circles = Al-compounds, squares = Ga-compounds, triangles = In-compounds; blue = Cu-based, red = Ag-based.

Conclusions

A systematic theoretical investigation of the refractive index of eighteen I–III–VI_2 ternary chalcopyrite semiconductors ($CuAlS_2$ to $AgInTe_2$) has been carried out using the Phillips–Van Vechten–Levine (PVL) dielectric theory. And based on the obtained results it can be concluded that the refractive index is an increasing function of the PVL compositional parameter $x = \langle n \rangle / \bar{\chi}$, varying from 2.35 for $CuAlS_2$ (x = 0.53) to 3.22 for $AgInTe_2$ (x = 1.39). A linear least-square regression relation, $n = 1.0212x + 1.8478$(R^2 = 0.9843), and a power-law relation, $n = 2.8946x^{0.3311}$(R^2 = 0.9875), both exhibits excellent predictive capability across the entire chalcopyrite family. Comparatively conventional models such as the Penn model and Ravindra relation show significantly weaker correlations confirming that the PVL parameter 'x' serves as a more reliable descriptor of optical behavior in these materials. Notably the calculated refractive indices show excellent match with available experimental and density functional theory data within a deviation margin of ± 0.02 validating the accuracy of the PVL-based approach. The observed power-law exponent of approximately one-third also suggests a meaningful volume-scaling relationship between the refractive index and the PVL parameter, indicating scope for deeper theoretical exploration. Overall, this work establishes a compact and physically grounded predictive framework for estimating the refractive index of

I–III–VI_2 chalcopyrites, which can be effectively utilized for material screening in nonlinear optical, photovoltaic, and infrared optoelectronic applications.

Acknowledgment

I would like to express my sincere gratitude to all those who have contributed to the successful completion of this research study titled "Theoretical Study of the Refractive Index of I–III–VI_2 Type Ternary Chalcopyrite Semiconductors on the Basis of PVL Theory." I am deeply indebted to my research guide and faculty members for their invaluable guidance, continuous encouragement, and constructive suggestions throughout the course of this study. Their expertise and mentorship played a vital role in the successful completion of this research.

Financial support and sponsorship

Nil.

Conflicts of interest

The authors declare that there are no conflicts of interest regarding the publication of this paper.

References

1. Phillips, J. C. (1970). Ionicity of the chemical bond in crystals. *Reviews of Modern Physics*, 42, 317–317.
2. Van Vechten, J. A. (1969). Quantum dielectric theory of electronegativity in covalent systems I. *Physical Review*, 182, 891–891.
3. Levine, B. F. (1973). Bond susceptibilities and ionicities in complex crystal structures. *The Journal of Chemical Physics*, 59, 1463–1463.
4. Penn, D. R. (1962). Wave-number-dependent dielectric function of semiconductors. *Physical Review*, 128, 2093–2093.
5. Ravindra, N. M., Auluck, S., & Srivastava, V. K. (1979). On the Penn gap in semiconductors. *Physica Status Solidi B*, 93, K155–K155.
6. Sharma, S. N., Bhar, R., & Ganguli, T. (2002). Optical properties of $CuInSe_2$ and related compounds. *Solar Energy Materials and Solar Cells*, 73, 363–363.
7. Tripathy, S. K. (2015). Refractive indices of semiconductors from energy gaps. *Optical Materials*, 46, 240–240.
8. Verma, A. S., & Kumar, A. (2012). Bulk modulus of cubic perovskites. *Journal of Alloys and Compounds*, 541, 210–210.
9. Newnham, R. E. (2005). *Properties of materials: Anisotropy, symmetry, structure*. Oxford University Press.
10. Reshak, A. H., & Auluck, S. (2003). Band structure and optical properties of the chalcopyrite compounds $CuAlX_2$ (X = S, Se, Te). *Physical Review B*, 68, 125101.
11. Shay, J. L., & Wernick, J. H. (1975). *Ternary chalcopyrite semiconductors: Growth, electronic properties, and applications*. Pergamon Press.
12. Kumar, P. R., & Verma, A. (2000). Phillips–Van Vechten–Levine parameters for I–III–VI_2 semiconductors. *Journal of Physics and Chemistry of Solids*, 61, 1671–1671.
13. Gorai, S. K., Parida, G., & Sharma, A. K. (2017). An empirical bulk modulus model of ternary chalcopyrite structure solids. *Methodology*, 10(3), 751–758.
14. Sharma, A. K., & Prasad, S. (n.d.). Ternary chalcopyrite: Most promising material of this century. *Advances in Science & Technology*, 19.
15. Sharma, A. K., Gorai, S. K., & Prasad, S. (2019). Relation of lattice energy with electronegativity and principal quantum number for ternary chalcopyrite semiconductors. *International Journal of All Research Writings*, 1(10), 37–41.
16. Sharma, A. K. (2025). Study of microhardness of $AgGaX_2$ (X = S, Se, Te) on the basis of Quantum ESPRESSO. *International Journal of Scientific Research in Multidisciplinary Studies*, 11(5).
17. Sharma, A. K. (2025). Lattice energy of $ZnXAs_2$ (X = Si, Ge, Sn) compounds: A density functional theory study using Quantum ESPRESSO. *Sciences*, 2(5), 69–73.
18. Sharma, A. K., Prasad, S., & Gorai, S. K. (2020). HOMO and LUMO approach of bulk modulus of ternary chalcopyrites. *Journal of Resource Management and Technology*, 11(3), 71–75.
19. Sharma, A. K., Prasad, S., & Gorai, S. K. (2019). An empirical relation for the calculation of ionicity of ternary chalcopyrite semiconductors.
20. Singh, P., et al. (2017). Ab initio studies of structural, electronic, optical, elastic and thermal properties of $CuGaTe_2$. *Semiconductors*, 51(5), 679–687.
21. Ghosh, A., Jana, S., Rani, D., Hossain, M., Niranjan, M. K., & Samal, P. (2024). Accurate prediction of band gaps and optical spectra of chalcopyrite semiconductors using dielectric-dependent hybrid functional. *Physical Review B*, 109, 045133.
22. Kumar, D., & Singh, D. (2024). Optical and electronic properties of chalcopyrite structured solids. *International Journal of Research and Analytical Reviews*, 11(2)
23. Xue, S., Ning, J., Zhang, B., Wu, Q., Zhang, F., & Zhang, W. (2022). Electronic structure and optical properties of $CdGeAs_2$: A DFT and HSE06 study. *Coatings*, 12(11), 1778.